Biomedicine & Pharmacotherapy 173 (2024) 116381

Contents lists available at ScienceDirect

Biomedicine & Pharmacotherapy

journal homepage: www.elsevier.com/locate/biopha

Curcumin encapsulated in milk small extracellular vesicles as a nanotherapeutic alternative in experimental chronic liver disease

Virginia Albaladejo-García [a,1], Laura Morán [b,1], Ana Santos-Coquillat [a,c], María I. González [a,c], Hui Ye [b], Elena Vázquez Ogando [d,e], Javier Vaquero [d,e], Francisco Javier Cubero [b,d,e], Manuel Desco [a,c,f,g,*], Beatriz Salinas [a,c,f,g,*]

[a] Unidad de Medicina y Cirugía Experimental, Instituto de Investigación Sanitaria Gregorio Marañón (IiSGM), Madrid 28007, Spain
[b] Departamento de Inmunología, Oftalmología y ENT, Facultad de Medicina de la Universidad Complutense de Madrid, Madrid 28040, Spain
[c] Unidad de Imagen Avanzada, Centro Nacional de Investigaciones Cardiovasculares (CNIC), Madrid 28029, Spain
[d] HepatoGastro Lab, Instituto de Investigación Sanitaria Gregorio Marañón (IiSGM), Madrid 28007, Spain
[e] Centro de Investigación Biomédica en Red de Enfermedades Hepáticas y Digestivas (CIBEREHD), Madrid, Spain
[f] Departamento de Bioingeniería, Universidad Carlos III de Madrid, Madrid 28911, Spain
[g] CIBER de Salud Mental, Instituto de Salud Carlos III, Madrid, Spain

ARTICLE INFO

Keywords:
nanoparticle
exosome
curcumin
drug delivery system
hepatic disease
extracellular vesicle

ABSTRACT

Curcumin is a natural molecule widely tested in preclinical and clinical studies due to its antioxidant and anti-inflammatory activity. Nevertheless, its high hydrophobicity and low bioavailability limit *in vivo* applications. To overcome curcumin's drawbacks, small extracellular vesicles (sEVs) have emerged as potential drug delivery systems due to their non-immunogenicity, nanometric size and amphiphilic composition. This work presents curcumin cargo into milk sEV structure and further *in vitro* and *in vivo* evaluation as a therapeutic nanoplatform. The encapsulation of curcumin into sEV was performed by two methodologies under physiological conditions: a passive incorporation and active cargo employing saponin. Loaded sEVs (sEVCurPas and sEVCurAc) were fully characterized by physicochemical techniques, confirming that neither methodology affects the morphology or size of the nanoparticles (sEV: 113.3±5.1 nm, sEVCurPas: 127.0±4.5 nm and sEVCurAc: 98.5±3.6 nm). Through the active approach with saponin (sEVCurAc), a three-fold higher cargo was obtained (433.5 μg/mL) in comparison with the passive approach (129.1 μg/mL). These sEVCurAc were further evaluated *in vitro* by metabolic activity assay (MTT), confocal microscopy, and flow cytometry, showing a higher cytotoxic effect in the tumoral cells RAW264.7 and HepG2 than in primary hepatocytes, specially at high doses of sEVCurAc (4%, 15% and 30% of viability). *In vivo* evaluation in an experimental model of liver fibrosis confirmed sEVCurAc therapeutic effects, leading to a significant decrease of serum markers of liver damage (ALT) (557 U/L to 338 U/L with sEVCurAc therapy) and a tendency towards decreased liver fibrogenesis and extracellular matrix (ECM) deposition.

1. Introduction

Chronic liver disease (CLD) is a major cause of morbidity and mortality worldwide, with more than 840 million people affected and 2 million deaths in 2020 [1]. Various causes of CLD may involve a progressive deterioration of liver function leading to fibrosis. Liver fibrosis

Abbreviations: sEVs, Small extracellular vesicles; sEVCur, loaded sEVs; sEVCurAc, loaded sEVs by active approach; ECM, Extracellular matrix; CLD, chronic liver disease; ROS, reactive oxygen species; DDS, Drug delivery systems; NPs, nanoparticles; PBS, phosphate-buffered saline; DLS, Dynamic light Scattering; NTA, Nanoparticle Tracking Analysis; TEM, Transmission Electronic Microscopy; RT, room temperature; FC, Flow Cytometry; SCy5, Sulfo-cyanine5 NHS ester; HPLC, high performance liquid chromatography; AM, attachment media; DMEM, Dulbecco's Modified Eagle Medium; FBS, Fetal Bovine Serum; DPBS, Dulbecco's phosphate-buffered saline; DAPI, 4′,6-diamidino-2-phenylindole; MTT, 3–4,5-Dimethylthiazol-2-yl-2,5-diphenyltetrazolium bromide; SEVSCy5-Cur, sEV fluorescent label and curcumin cargo; SPF, pathogen-free; CCl4, carbon tetrachloride; AST, aspartate aminotransferase; ALT, alanine aminotransferase; PFA, paraformaldehyde; H&E, hematoxylin & eosin; SR, red staining; SD, standard deviation; SEM, standard deviation of the mean; HSCs, Hepatic stellate cells.

* Corresponding author at: Unidad de Medicina y Cirugía Experimental, Instituto de Investigación Sanitaria Gregorio Marañón (IiSGM), Madrid 28007, Spain.
E-mail addresses: manuel.desco@uc3m.es (M. Desco), bsalinas@pa.uc3m.es (B. Salinas).

[1] These authors contributed equally.

https://doi.org/10.1016/j.biopha.2024.116381
Received 7 November 2023; Received in revised form 27 February 2024; Accepted 29 February 2024
Available online 7 March 2024

represents the excessive accumulation of ECM proteins, mostly collagen, that occurs in many types of CLD. Advanced liver fibrosis results in cirrhosis, liver failure, and portal hypertension and often requires liver transplantation [2]. The pathology of liver fibrosis is associated with increased oxidative stress, regardless of the origin of the liver pathology [3]. The excess of reactive oxygen species (ROS) and the imbalance between oxidants and antioxidants give rise to oxidative stress, which can lead to the degradation of cellular components. Although our knowledge of the cellular and molecular mechanisms of liver fibrosis has greatly advanced in the last decades, the reversibility of advanced liver fibrosis in patients is still an issue, which has stimulated researchers to work on the development of antifibrotic drugs. Therefore, there is a need for therapeutic interventions that might be effective in experimental and clinical liver fibrosis.

Curcumin is a natural polyphenol molecule extensively employed as a treatment for multiple diseases due to its beneficial properties, attributed to its anti-oxidative, anti-inflammatory, immunomodulatory, and protective properties [4,5]. This natural compound has been widely investigated in the treatment of several liver diseases, including non-alcoholic and alcoholic steatohepatitis [6–8]. Curcumin inhibits inflammatory molecules and enhances antioxidant defense, protecting against liver illnesses as well as cardiovascular, neurological, or tumoral damage [9–12]. Despite the promising application of curcumin as an efficacious and safe compound for therapy, some limitations still need to be addressed, such as its poor bioavailability associated with its low solubility, limited absorption, rapid metabolism, and rapid elimination [13]. To overcome these limitations, several methodologies have been developed to improve drug bioavailability and enhance drug delivery to target tissues. Thus, the use of novel nanoparticle-based drug delivery systems has emerged as one promising tool [14,15].

In the development of novel drug delivery systems (DDS) based on nanometric platforms, small extracellular vesicles (sEVs) are emerging as interesting natural nanoplatforms. sEVs are natural vesicles with a nanometric size (30–150 nm), physiologically released by the cells [16]. They are well-known for their implication in the exchange of lipids, proteins, mRNA or effector molecules between cells [17]. In addition, in the last decade these vesicles have been widely employed in the development of imaging agents for diagnosis [18,19] and as natural nanoparticles (NPs) for therapy [20]. Their intrinsic characteristics make them appropriate candidates for their use as DDS [21]. On the one hand, their structure based on a bilipid membrane allows the incorporation of hydrophilic molecules into their aqueous lumen as well as hydrophobic drugs into their lipidic membrane, similar to that of synthetic liposomes [22,23]. On the other hand, their natural origin reduces possible toxicity and immunogenicity [24]. Finally, from a chemical point of view, the richness of their biochemical composition provides numerous functional groups that facilitate possible structural modifications or biofunctionalizations.

sEVs are secreted by a number of different cells, and they can be isolated from different biological fluids such as blood, urine, and milk [24–26]. Among all types of natural NPs, milk derivate sEVs are a potentially interesting resource due to their scalability, low cost and reduced immunogenicity [24]. Previous studies by our group demonstrated the promising application of goat milk sEVs as natural NPs in inflammatory processes, as well as their high hepatic uptake [18,27].

The aim of this work was to develop a novel DDS for curcumin by employing goat milk sEVs as nanovehicles (sEVCurPas and sEVCurAc). In vitro and in vivo validation as a therapeutic system is also presented in a model of experimental liver fibrosis.

2. Materials and methods

2.1. Milk sEV isolation

sEVs were obtained following previous protocols developed by our group [18]. Briefly, sEVs were isolated and purified from goat semi-skimmed milk (El Cantero de Letur, Albacete, Spain) by differential centrifugation at 4ºC using a centrifuge instrument Avanti J-30I (Beckman Coulter, Brea, CA, USA), rennet and size exclusion chromatography. To remove fat globules and milk casein, milk was centrifuged 10 min at 5,000 x g and mixed with microbial rennet (Ultzama, Navarra, Spain). The supernatant was sequentially centrifuged for 10 min at 5, 000 x g, 35 min at 13,000 x g, and 15 min at 35,000 x g to eliminate large vesicles and cell debris. Finally, milk whey was ultracentrifuged at 100, 000 x g for 70 min to precipitate the sEVs. The resultant pellet was washed three times with phosphate-buffered saline (PBS 1X) and purified by PD-10 size-exclusion columns (Cytiva, Merck, Germany). sEVs were concentrated by ultracentrifugation at 100,000 x g for 90 min and dispersed in 100 μL PBS 1X and stored at −80°C until used (Scheme S1).

Protein content of sEVs was quantified by Bradford Coomassie methodology (Merck, Germany) and measured by a microplate-reader (680 XR, BIO-RAD, Hercules, California, USA).

2.2. Encapsulation of curcumin in milk sEVs structure

2.2.1. Passive methodology (sEVCurPas)

For the passive incorporation of curcumin into the vesicle structure (sEVCurPas), 200 μg of sEVs were mixed with 1000 μg of curcumin (Merck, Germany) in 1 mL of Phosphate-buffered saline (PBS) (Gibco, Life Technologies, Madrid, Spain). As control samples, sEVs were also exposed to similar reaction conditions without curcumin. The samples were incubated at 37ºC in agitation (300 rpm) and dark conditions during 90 min for passive approach. Then, each sample was purified by PD-10 size exclusion columns, collecting the initial 3 mL of the sample for further physicochemical characterization.

2.2.2. Active methodology (sEVCurAc)

Active cargo of the curcumin in the sEV structure (sEVCurAc) was achieved by means of saponin (Merck, Germany) by mixing 200 μg of sEVs with 1000 μg of curcumin, and 0.2% of saponin detergent in 1 mL of PBS 1X. As controls samples (sEVAc), we performed the same steps above without adding curcumin. In both assays, we obtained a homogeneous solution by using the vortex for 10 s. Then, each sample was purified by PD-10 size exclusion columns, collecting the initial 1.5 mL of the sample to for its physicochemical characterization.

2.3. Physicochemical characterization

2.3.1. Dynamic Light Scattering (DLS)

Hydrodynamic size of the samples was measured in a Zetasizer Nano ZS (Malvern Instruments, Malvern, UK). sEVs were diluted in 1 mL of PBS 1X (1:250) and filtered using a 0.45 μm filter. Size distribution was analyzed at 25°C according to the manufacturer's instructions.

2.3.2. Nanoparticle tracking analysis (NTA)

NTA was performed using a Nanosight NS300 instrument equipped with a 532 nm green laser and sCMOS camera (Malvern Instruments, Malvern, UK). To define the size and concentration of the particles, the samples were diluted appropriately in PBS 1X solution and filtered by 0.45 μm filter. Five videos were recorded under 0.9 cP (water) and 25ºC conditions. Real-time concentration (particles/mL), mean, mode and median of the extracellular vesicles were analyzed by NTA 3.4 Build software.

2.3.3. Transmission electron microscope (TEM)

sEV morphology and structure were characterized by TEM employing a JEOL JEM-1010 (JEOL, Japan) in Centro Nacional de Microscopía Electrónica (Madrid, Spain). Samples were prepared by diluting sEVs in PBS 1X (1:5) and filtered by 0.45 μm. A drop was put on a 200 mesh Formvar-coated copper grid previously negative staining with uranylacetate (2%) by glow discharge. Images were acquired at 100 KV by a Megaview II camera and processed by digital micrograph software.

2.3.4. Nanophotometry

Curcumin incorporation into sEV structure was assessed by absorbance employing a NanoPhotometer OD600 equipment (Implen GmbH, Germany) at room temperature (RT). sEVCurPas, sEVCurAc and curcumin-free sEVAc were diluted (1:5) ratio in PBS 1X to do a measurement in triplicate following the manufacturer's instructions. As negative control, PBS 1X was used. Between measurements, the system was cleaned with distilled water. A standard curve of curcumin in a range of 4 – 1000 μg/mL measured at 420 nm was plotted to evaluate the incorporation of curcumin.

2.3.5. Flow cytometry (FC)

sEV based nanoconjugates were processed in a Flow Cytometer equipment (Beckman Coulter, Brea, CA, USA) at RT and 405 and 488 nm laser excitation for curcumin self-fluorescence detection and 633 nm laser excitation for Sulfo-Cyanine5 NH ester (SCy5) fluorescence detection. Data was evaluated by Gallios Software. Fluorescence data was quantified and evaluated by FlowJo™ v10.7 software.

2.3.6. High Performance Liquid Chromatography (HPLC)

Purity of the SCy5 fluorescently labelled and curcumin encapsulated nanovehicle (sEVSCy5-Cur) was confirmed by HPLC analysis Agilent 1200 series (Agilent Technologies, Santa Clara, CA, USA) equipped with a UV–VIS detector (425 nm for curcumin and 600 nm for SCy5) and SEC-3000 column (300 ×7.8 mm; Phenomenex Inc., Torrance, CA, USA). An isocratic gradient of PBS 1X with a flow rate of 0.5 mL/min for 50 min was employed. Gina Star (Microbeam S.A., Madrid, Spain) Chromatography Software was employed for data acquisition, evaluation, integration, and system control.

2.4. In vitro curcumin release from sEVCurAc

Release of curcumin from sEVCurAc was *in vitro* assessed in aqueous solution at pH 7.4 by using 0.1 M $NaHCO_3$ buffer. sEVCurAc were incubated at 37ºC and 300 rpm and evaluated at 0, 1, 3, 6, 24, 48, 72, 144, 168, 192 and 216 h. For each time point, 100 μL of sample were purified via Amicon 100 kDa (Merck, Germany) following manufacturer's instructions. Then, we measured the absorbance of the pellet and supernatant by NanoPhotometer OD600 equipment. To calculate the percentage of curcumin concentration, the curcumin content in the supernatant was divided by the combined curcumin concentration of the supernatant and pellet.

2.5. Cell culture

Primary hepatocytes were freshly isolated from C57/BL6 wildtype mice by a two-step protocol for hepatic perfusion from the inferior cava vein [27]. Briefly, the liver was first perfused with Hank's Balanced Salt Solution (without phenol-red, calcium or magnesium; Gibco, ThermoFisher Scientific, Waltham, MA, USA), containing 0.2 mM EGTA, 10 U/mL heparin and 10 mM HEPES (pH 7.4). Then, perfusion was performed with Williams E Medium (Gibco, ThermoFisher Scientific, Waltham, MA, USA), containing 10 mM HEPES (pH 7.4) and 0.4 mg/mL collagenase type IV from Clostridium histolyticum (Merck, Germany). Cells were resuspended, after filtering the digested liver through a 100 μm-pore cell strainer, in attachment media (AM) (DMEM:F12 with 10% FBS supplemented with 5 mM sodium pyruvate, 2 mM L-glutamine, 0.05% $NaHCO_3$, 20 mM HEPES, 0.12% glucose, 0.02% BSA, 100 U/mL penicillin, and 100 μg/mL streptomycin). Next, the mixture was centrifuged at 50 x g, and purified with density gradient centrifugation in an isotonic solution of Percoll (GE Healthcare Bio-Sciences AB, Sweden). After a wash in AM with a 50 x g centrifugation, cells were cultured in AM at 37ºC in a humidified incubator containing 5% CO_2.

RAW 264.7 cells (ATCC® TIB-71™) and HepG2 cells (ATCC® HB 8065™) were provided by American Type Culture Collection. Cells were cultured in high glucose Dulbecco's Modified Eagle Medium (DMEM) (Merck, Germany) supplemented with 10% Fetal Bovine Serum (FBS) (Cultek, Madrid, Spain) and 1% of penicillin/ streptomycin/ anfotericin B (Cultek, Madrid, Spain) as antibiotics at 37ºC in a humidified incubator containing 5% CO_2.

2.6. Confocal microscopy

In vitro uptake of the nanoconjugate was visualized by confocal imaging. Cells were seeded in 24-well plates at a density of 3×10^4 cells for RAW 264.7 and HepG2 and 9×10^4 per well over a circular coverslip of 12 mm diameter (Marienfeld Superior, Germany) in primary hepatocytes. Four hours after seeding, cells were treated with 0.5 μg/mL or 5 μg/mL of sEVCurAc diluted in Dulbecco's phosphate buffered saline (DPBS) (Merck, Germany). Cells were incubated with sEVCurAc at 37ºC and 5% of CO_2 for 5 min, 1 h, 4 h and 24 h. After those incubation time points, we gently removed the medium and added 2% paraformaldehyde for 10 min at RT to fix cells. Subsequently, well plates were washed once with 1 mL of DPBS and stored at 4ºC until labeling. Each condition was performed in triplicate. In all experiments, cells without treatment were used as control.

In the case of primary hepatocytes and HepG2 cells, a preconditioning step was included. Therefore, before cell seeding over treatment coverslips, rat tail collagen (Merck, Germany) was added to the coverslips to allow the adhesion and growth of these cells. Briefly, we prepared a solution (1:1000) of collagen in DPBS. We added 500 μL of solution in each coverslip and then UV sterilized for 30 min and incubated for 1 h at 37ºC. Then, we removed the excess of collagen and washed once with DPBS. We then removed the DPBS and seeded and incubated the cells with the sEVCurAc following the protocol described above.

2.7. Immunofluorescence labelling

Fixed cells were stained with 300 μL/well of phalloidin -ifluor 555 (ab176756, Abcam, Cambridge, UK) for actin cytoskeleton, and 4′,6-diamidino-2-phenylindole (DAPI) (Merck, Germany) for nuclei, during 30 min at RT in agitation and darkness conditions. Then, we washed twice with PBS 1X. Subsequently, each coverslip was mounted over a slice with mounting medium (DAKO, Merck, Germany) overnight at 4ºC. Samples were excited by 405 (DAPI), 488 (curcumin), 555 nm (phalloidin) and 635 nm (SCy5) laser with LEICA-SPE upright fluorescence microscope (Leica, Germany). Images were analyzed by LCS 15.37 software Images were processed by Fiji ImageJ software (U. S. National Institutes of Health, Bethesda, MD, USA).

2.8. MTT assay

3-(4,5-Dimethylthiazol-2-yl)-2,5-diphenyltetrazolium bromide assay kit (MTT) (Merck, Germany) was employed in the assessment of *in vitro* cytotoxicity of sEVCurAc at 24 h and 48 h in RAW264.7, primary hepatocytes and HepG2. RAW264.7 or HepG2 were seeded on 96-well plates (Corning, NY, USA) at a concentration of 1×10^4. In the case of primary hepatocytes, cells were seeded at a density of 2×10^4 cells on 96-well plate previously treated with collagen. Cells were treated with 0.5 μg/mL or 5 μg/mL of sEV control (sEV)or loaded sEVs sEVCurAc at 37ºC and 5% of CO_2. After treatment time points (24 h and 48 h), 10 μL of MTT reagent were added in each well and well-plates were incubated 2 h at 37ºC. Then, the media was removed, and formazan crystals were dissolved by adding 100 μL of DMSO. Then, absorbance was measured (BIO-RAD, 680 XR) at 540 nm. Each condition was performed in quadruplicate.

2.9. Cell uptake assessment of sEVCurAc by FC

FC was employed for the quantification of the *in vitro* incorporation of sEVCurAc in cancer cell lines RAW 264.7 and HepG2 at 1 h, 4 h and

24 h of incubation. Briefly, 1.5 $\times 10^5$ RAW 264.7 or 2 $\times 10^5$ HepG2 cells were seeded in 12- well plates (Corning, NY, USA). Cells were treated with 5 μg/mL of sEVCurAc diluted in DPBS. Cells were incubated at 37ºC and 5% of CO2 for 1 h, 4 h and 24 h. After that, cells were trypsinized using EDTA-trypsin (Merck, Germany) for 10 min and then, well plates were neutralized by FBS-depleted DMEM. All volume was recovered in flow cytometry tubes (Beckman Coulter, Brea, CA, USA) and centrifuged 5 min at 600 x g. Subsequently, we removed supernatant and washed once with 1 mL of DPBS. Then, tubes were centrifuged 5 min at 600 x g. We removed supernatant again and resuspended in 250 μL of DPBS in triplicate. Blank control and single staining control groups were set up. Each tube was evaluated during 5 min by Gallios Software. Data were analyzed by FlowJo™ v10.7 software.

2.10. Fluorescent labelling of sEV (sEVSCy5-Cur)

In vivo biodistribution of sEVCurAc was carried out by non-invasive optical imaging. For this purpose, the sEVCurAc systems were fluorescently labelled with the commercial dye SCy5 following protocols previously described by our group. For that, 200 μg of sEVs were mixed with 2 μL of 16.9 mM SCy5 (Lumiprobe, GmbH, Hannover, Germany) for 60 min at 37ºC and pH 8.5 following previous protocols of the group [27]. The final product was purified using Slide-A-Lyzer™ G2 Dialysis Cassettes (3.5 K MWCO, 0.5 mL, ThermoFisher Scientific, Waltham, MA, USA) for 24 h and concentrated by Amicon® Ultra-2 mL 100 kDa Centrifugal Filters (Merck-Millipore, USA). The resulting product was encapsulated with curcumin (sEVSCy5-Cur) following the active protocol in presence of saponin, previously described in section Active methodology (sEVCurAc).

2.11. In vivo optical imaging of sEVSCy5-Cur

In vivo probe biodistribution was evaluated by optical imaging using an IVIS® Lumina III *in vivo* Imaging System (Perkin Elmer, Waltham, MA, USA) employing a spectral unmixing protocol for SCy5 fluorophore. Mice were kept anesthetized with 2% isofluorane in 100% of O_2 via a facemask during the whole *in vivo* imaging procedure with an anesthesia System XGI-8 (100 V). Images were taken after 24 h, 48 h and 72 h of the intravenous injection of the probe ($5.56\times10^9 \pm 1.85\times10^7$ particles, PBS 1X, n=3). Analysis and quantification of the images were carried out with Living Image® 4.4 software (Perkin Elmer, Waltham, MA, USA). After last time point (72 h) organs of interest were harvested and *ex vivo* imaged (heart, lungs, liver, spleen, kidneys and intestines) and quantified by average radiant efficiency. Data were expressed as mean ± SD, in (p/s/cm2/sr)/(μW/cm2).

2.12. Western blot analysis

Liver lysates were separated by SDS-PAGE Handmade gels containing 5% polyacrylamide stacking gel and separating gel that range from 8% to 15% according to the molecular weight of the proteins were used; proteins were transferred to 0.45 μm or 0.22 μm PVDF membranes (BioRad, Madrid, Spain). Membranes were incubated with the appropriate first antibody (NQO1 sc-23793 and NRF2 CST12721S) and horseradish peroxidase (HEP)-conjugated secondary antibodies. Immunocomplex was detected using Amersham ECL Prime (GE, Healthcare, Amersham, UK).

2.13. Mouse model of liver fibrosis

All experimental procedures with animals conformed to EU Directive 2010/63EU and Recommendation 2007/526/EC, found in RD 53/2013. Animal protocols were approved by the Comité de Ética en Experimentación Animal de la Universidad Complutense de Madrid and the Animal Protection Area of the Comunidad Autónoma de Madrid (PROEX 125.1/20).

Mice were housed in a pathogen-free (SPF) animal facility and kept on a 12-h light/dark cycle at constant temperature and humidity and normal chow diet. Wild type female and male 129 s/BL6 mice at the age of 8- to 12-week-old were chemically induced liver injury by the administration of repeated intraperitoneal injections of carbon tetrachloride (CCl_4) [0.6 mL/kg] twice per week for 28 days. Corn oil was used as vehicle. 8 days after the start of CCl_4 administration, mice were treated intravenously with a total of 90 μg sEVCurAc divided into 3 different doses (3 administrations of 30 μg sEVCurAc) administered for the last 20 days every 5 days. All mice were sacrificed 48 h after the last injection.

Blood samples were extracted from cava vein and centrifuged at 12,000 x g during 10 min at 4ºC. To evaluate liver damage, levels of serum parameters of aspartate aminotransferase (AST) and alanine aminotransferase (ALT) were analyzed in the Central Laboratory in Gregorio Marañón Research Health Institute of Madrid (ilSGM).

2.14. Ex vivo histology

Liver samples were fixed with 4% paraformaldehyde (PFA) (AppliChem, Barcelona, Spain) and embedded in paraffin for histological evaluation using hematoxylin & eosin (H&E) and Sirius Red staining (SR). Photomicrographs of stained sections were taken in a 20x magnification in an optical microscope (Nikon Eclipse Ci, Tokyo, Japan). The percentage of positive area with both staining's was quantified using free NIH ImageJ software (National Institutes of Health, Bethesda, MD, USA).

2.15. Statistical analysis

Data was analyzed by Prism software 6 (Graph pad, Inc., San Diego, CA, USA) and performed by One-Way ANOVA and Tukey's post-test for physicochemical characterization or Two-Way ANOVA and Tukey's post-test for *in vitro* assessments. Data were represented as mean ± standard deviation (SD). P-values <0.05 were considered significant.

Statistical analysis of *in vivo* data consisted of One Way ANOVA followed by Tukey post-hoc tests using GraphPad Prism version 8.0 software (San Diego, CA, USA). A p value <0.05 was considered statistically significant. Data were expressed as mean ± standard deviation of the mean (SEM).

3. Results

3.1. Verification of curcumin encapsulation and physicochemical characterization

FC (Fig. 1. A) confirmed curcumin incorporation into vesicles structure both in sEVCurPas and sEVCurAc. Further quantitative assessment by fluorescent nanophotometry (Fig. 1. B) confirmed threefold higher incorporation of curcumin when employing active approach with saponin (433.5 μg/mL) than with passive approach (129.1 μg/mL).

A complete physicochemical characterization of the nanosystems was carried out to assess the effect of the loading methodology into the vesicle structure after the incorporation of the drug. In both cases TEM images confirmed charged sEVs, sEVCurPas and sEVCurAc, maintained size and typical 'cup-shape' morphology, compared to control sample (Fig. 2. A). Hydrodynamic size assessed by DLS showed that encapsulated sEVs presented a smaller hydrodynamic size compared to control with statistically significant differences (sEV: 130.0±6.7 nm, sEVCurPas: 120.5±0.3 nm and sEVCurAc: 106±4.1 nm) (Fig. 2. D) with PdI values of 0.122±0.034 and 0.143±0.026 for sEVCurPas and sEVCurAc respectively [28,29]. NTA showed a similar nanometric size in the encapsulated samples in comparison to the curcumin-free sEVs (sEV: 113.3±5.1 nm, sEVCurPas: 127.0±4.5 nm and sEVCurAc: 98.5 ±3.6 nm) (Fig. 2. C) and slight reduction in NPs concentration after incorporation of the drug in their structure (sEV: $3.31\times10^8 \pm 2.56\times10^7$

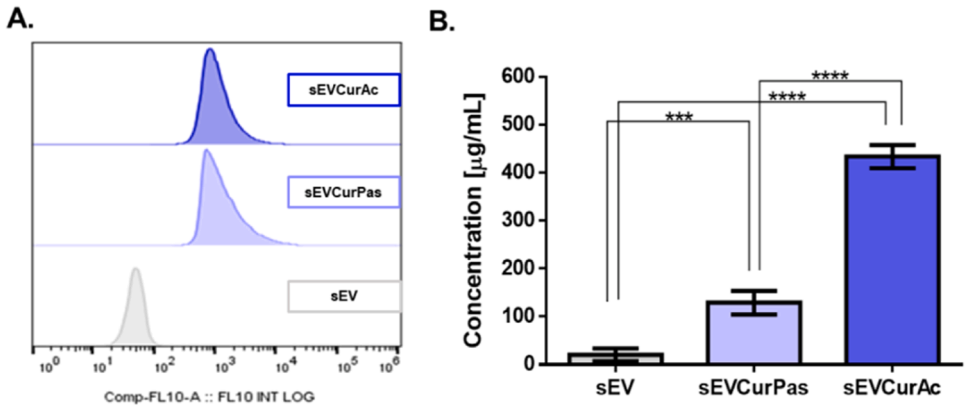

Fig. 1. Curcumin incorporation into control sEVs (control), sEVCurAc (active) and sEVCurPas (passive) samples analyzed by A) FC analysis, and B) nanophotometer. **** $p<0.0001$.

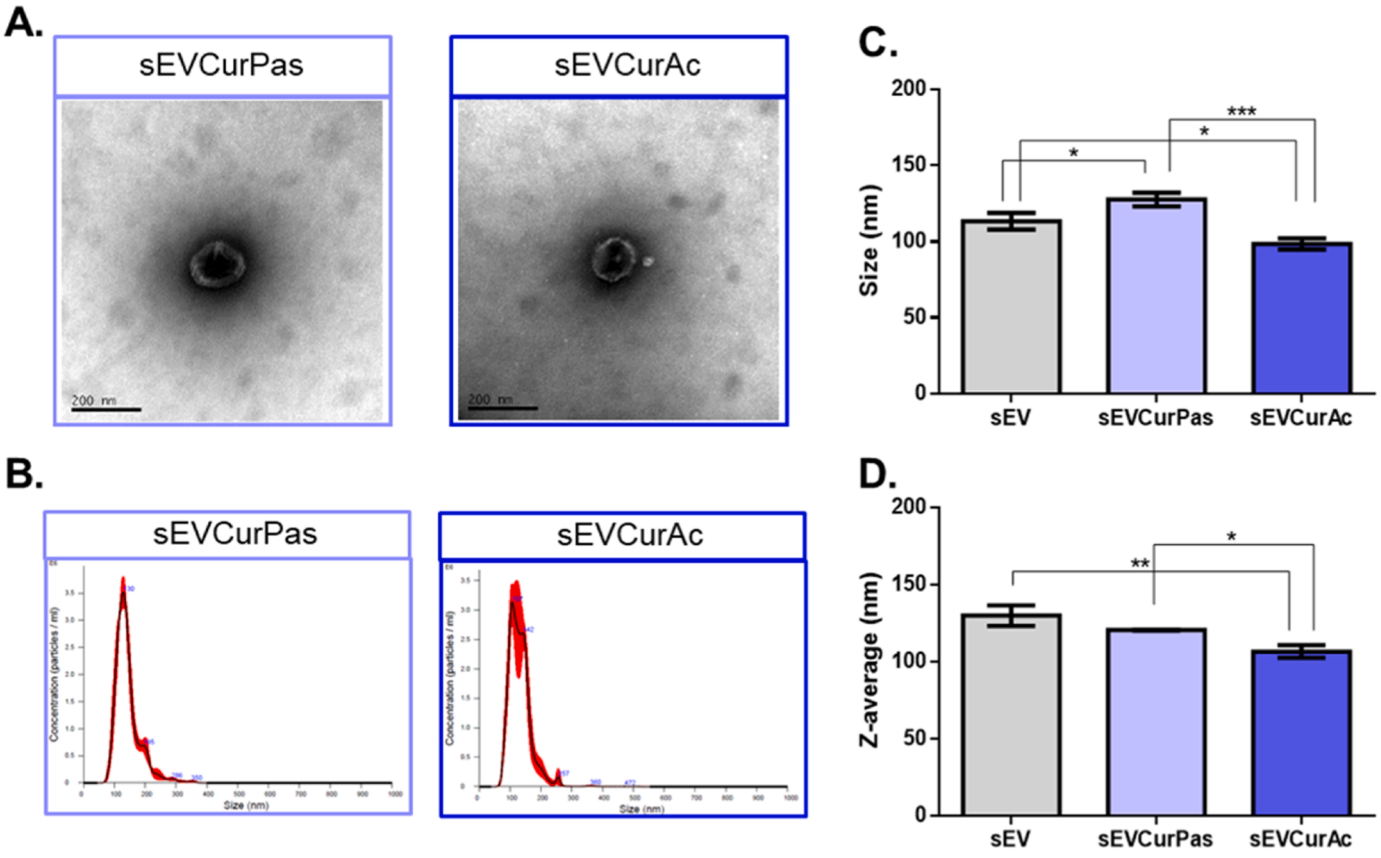

Fig. 2. Morphological characterization of the sEVCurPas, sEVCurAc and sEV (control). Size and shape evaluation by A) TEM, B) and C) NTA and D) DLS. *** $p<0.0008$, ** $p<0,0022$.

particles/mL, sEVCurPas: $2.31\times10^{8} \pm 1.31\times10^{7}$ particles/mL and sEVCurAc: $2.30\times10^{8} \pm 3.34\times10^{7}$ particles/mL) (Fig. 2. B).

3.2. Longitudinal assessment of curcumin release from sEVCurAc

Longitudinal assessment of the curcumin release by means of the percentage of curcumin concentration in the supernatant revealed an increase of the drug release along time (Fig. 3. A) compared to baseline values. During the initial 4–48 h the release of curcumin showed a slow kinetic, but the curcumin concentration of the supernatant, and thus the presence of curcumin, showed an intense sharply increased from 48 h to 144 h until 216 h.

In addition, we performed a fluorescence spectrum analysis by fluorospectrometry (Fig. S1) to verify if fluorescence properties, and therefore structural morphology of the curcumin, were kept after loading into the sEVs. Both, free curcumin and sEVCurAc, showed the same fluorescence plot confirming that loaded NPs maintained structural and optical properties of the curcumin structure.

3.3. In vitro evaluation of sEVCurAc

In vitro evaluation of the nanosystem in tumour-related (RAW 264.7 and HepG2) and control cells (primary hepatocytes) showed different patterns in the presence of high (5 µg/mL) or low (0.5 µg/mL) doses of

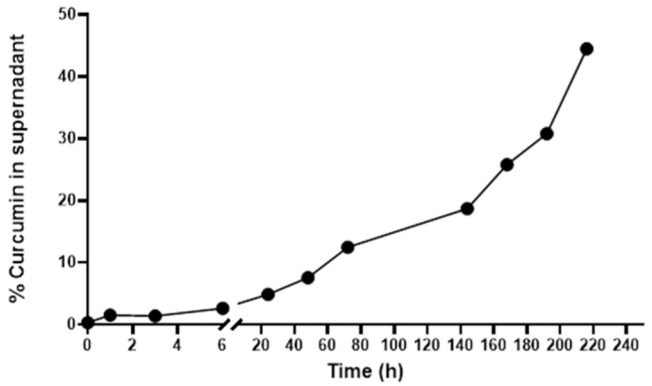

Fig. 3. A. Release of encapsulated curcumin from sEVCurAc at pH 7.4 at different times points (0, 1, 3, 6, 24, 48, 72, 144, 168, 192 and 216 h).

sEVCurAc (Fig. 4 and Fig. S2).

None of the cell populations showed significant toxic effects at the low dose (0.5 μg/mL) compared to the vehicle (sEV) at any time point (Fig. 4. A and Fig. S. 3. A). However, for drug-loaded vesicles, sEVCurAc, a significant cytotoxic effect was observed for RAW 264.7 and primary hepatocytes compared to control cells at 48 h. Only HepG2 cells showed no reduction in viability. Instead, a significantly higher viability was observed at 48 h in the presence of both vehicle and loaded sEVs (sEVCurAc) (Fig. 4. A).

At the high dose (5 μg/mL), all cell lines treated with EVsCurAc showed significant cytotoxic effects compared to vehicle-treated cells (sEVs without curcumin) and untreated control cells. This effect was observed both at 24 h and 48 h (Fig. 4 and Fig. S2. B). More specifically, RAW 264.7 cells showed higher viability at 24 h in the presence of vehicle (sEV) compared to the control group. The HepG2 cell line showed an abrupt decrease in viability at the higher dose at 24 h and 48 h up to 35% and 15% respectively (Fig. 4. A and B). In the case of HepG2, vehicle sEVs did not seem to affect the viability of HepG2 in any way compared to control cells. Finally, in the case of primary hepatocytes, viability was reduced up to 50% and 80% at 24 h and 48 h in the presence of high dose of sEVCurAc showing a significant reduction in the viability compared to the effect of the vehicle without the curcumin (Fig. 4. A and B).

In vitro qualitative evaluation of sEVCurAc internalization by confocal microscopy (Fig. 5. A and Fig. S3) confirmed the presence of sEVCurAc (488 nm laser) in all cell lines (RAW 264.7, HepG2 and primary hepatocytes), with a dispersed cytoplasmatic distribution at both low (0.5 μg/mL) and high doses (5 μg/mL). Compared to control conditions, RAW 264.7 proliferate less when in contact with sEVCurAc, with a significant effect found with the higher dose where very few rounded cells could be found in accordance with their low metabolic activity results (Fig. 4). HepG2 cells showed similar behaviour with the higher dose with more prevalent morphological changes as the cells lost the elongated phenotype. sEVCurAc produced a cytotoxic effect in all tested cells being noticeable in a time- and dose- dependent manner (Fig. 5. A. and Fig. S3).

In the FC analysis based on curcumin fluorescence at higher doses, both, RAW 264.7 and HepG2 cell populations (Fig. 5. B and C) were 100% positive for the curcumin (sEVCurAc) at every time point indicating the uptake of the probe, showing a longitudinal and statistically significant increase in MFI over the time. However, this uptake was higher in the case of RAW cells at each time point, especially at 24 h (~100000 MFI for HepG2 and ~150000 MFI for RAW 264.7 cells).

3.4. *In vivo tracking of sEVSCy5-Cur by optical imaging*

In vivo imaging of the nanovesicles was carried out with the fluorescent version of sEVCurAc (sEVSCy5-Cur). A previous characterization (Fig. S4) of the fluorescent compound by HPLC confirmed the high purity of the sample, by the presence of a single peak in both HPLC chromatograms (254 nm and 600 nm) at 10 min, with no secondary peaks from the fluorophore or free curcumin (Fig. S4. B). FC confirmed the presence of curcumin and dye colocalization (Fig. S4. C).

Longitudinal *in vivo* imaging of healthy mice confirmed the hepatic accumulation of sEVSCy5-Cur from the initial timepoint at 24 h, showing hepatic accumulation of the nanosystem at 48 h and 72 h post-injection (Fig. S5 and Fig. 6). This accumulation of sEVCurSCy5 in liver tissue was confirmed by the *ex vivo* analysis (Fig. 6) with a result of 2.84e+08 ±2.20e+08 (p/s/cm2/sr)/(μW/cm2).

3.5. *In vivo assessment of the therapeutic effect of sEVCurAc in an acute hepatic model*

Finally, sEVCurAc was evaluated as a therapeutic drug delivery system in an animal model of acute liver disease induced by CCl_4 injection (Fig. 7. A), taking advantage of the natural migration of sEVs into liver tissue [5,18,30].

Histological analysis by H&E and Sirius Red staining showed that control CCl_4 model animals displayed higher collagen deposition in the liver than the group treated with sEVCurAc, indicating a significant reduction in fibrogenesis (Fig. 7. B). Interestingly, control animals did not show differences in their liver tissue morphology despite being treated with sEVs; thus, sEVCurAc had no effect on healthy animals. Necrotic foci assessed by H&E were evaluated and plotted (Fig. 7. C), and collagen deposition was analysed using SR (Fig. 7. D), staining showed a clear trend towards a reduction in necrotic foci and ECM deposition after sEVCurAc treatment. Next, we evaluated serum markers of liver injury (AST, ALT). Notably, a tendency towards decreased levels of AST (Fig. 7. E) and a significant decrease in ALT (Fig. 7. F) levels were observed in sEVCurAc-treated livers of fibrotic CCl_4-induced mice. RNA expression analysis of extracellular matrix components such as Collagen IA1 and alpha-smooth muscle actin on liver tissue showed a significant decrease in collagen deposition (A) in tissue from damaged livers treated

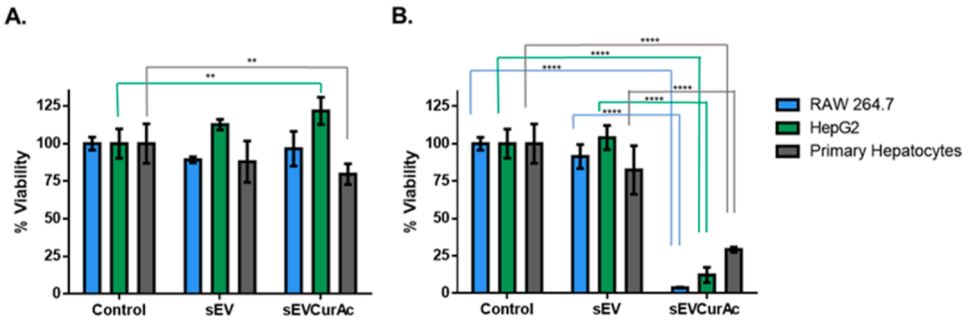

Fig. 4. Viability evaluation by MTT assay of sEVCurAc and vehicle (sEV) with RAW 264.7, HepG2 and primary hepatocyte cells at 48 h. at low doses (0.5 μg/mL) (A) and high doses (5 μg/mL) (B) of Exo or sEVCurAc. **** $p < 0.0001$.

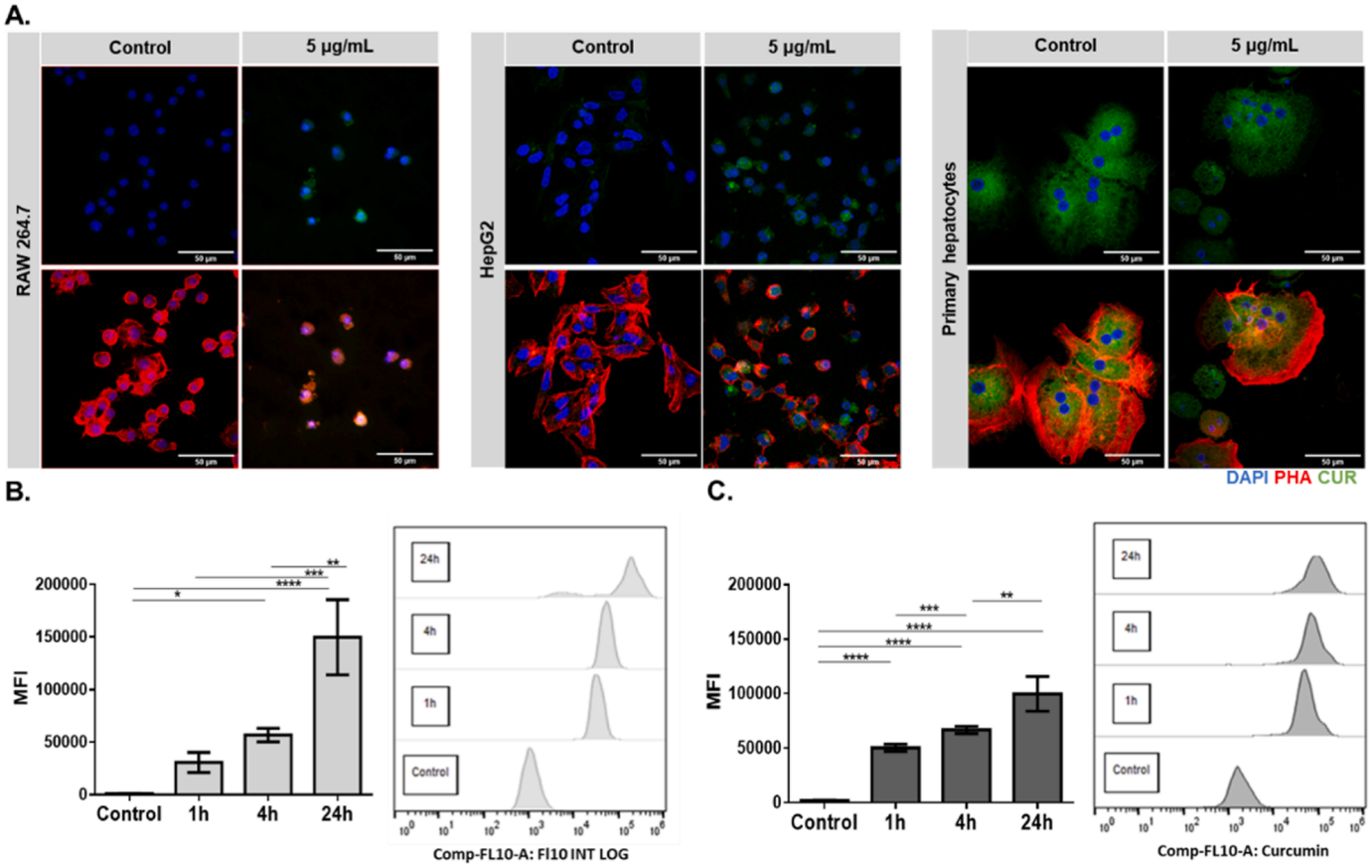

Fig. 5. Uptake of encapsulated sEVs (sEVCurAc). A. Confocal microscopy of sEVCurAc in RAW 264.7, HepG2 and primary hepatocytes cells at 5 µg/mL at 24 h. The scale bar corresponds to 50 µm. FC evaluation of sEVCurAc at 1 h, 4 h and 24 h and 5 µg/mL in RAW 264.7 (B) and HepG2 (C). **** $p < 0.0001$.

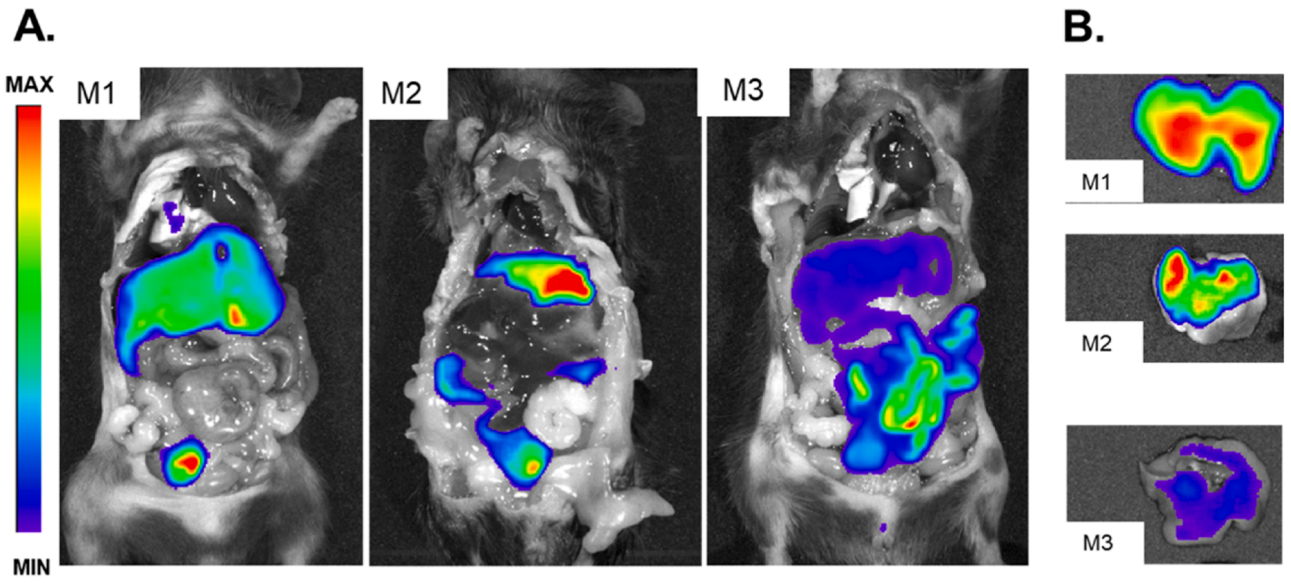

Fig. 6. *Ex vivo* biodistribution of sEVSCy5-Cur 72 h post administration in wild type mice by optical imaging in full animal (A) and excised liver (B).

with sEVCurAc (Figure S6). In addition, although sEVCurAc had no direct effect on the phosphorylation of Nrf2, one of the target genes of Nrf2, previous assessment of NQO1 by WB showed that NQO1 appears to be significantly attenuated by sEVCurAc treatment after CCl4 (Figure S7).

4. Discussion

This work presents the use of milk sEVs as a natural nanometric DDS for the natural anti-inflammatory and antioxidant molecule curcumin. Previous studies have demonstrated the use of milk EVs without any toxicity associated [19,31]. To carry out encapsulation and avoid any

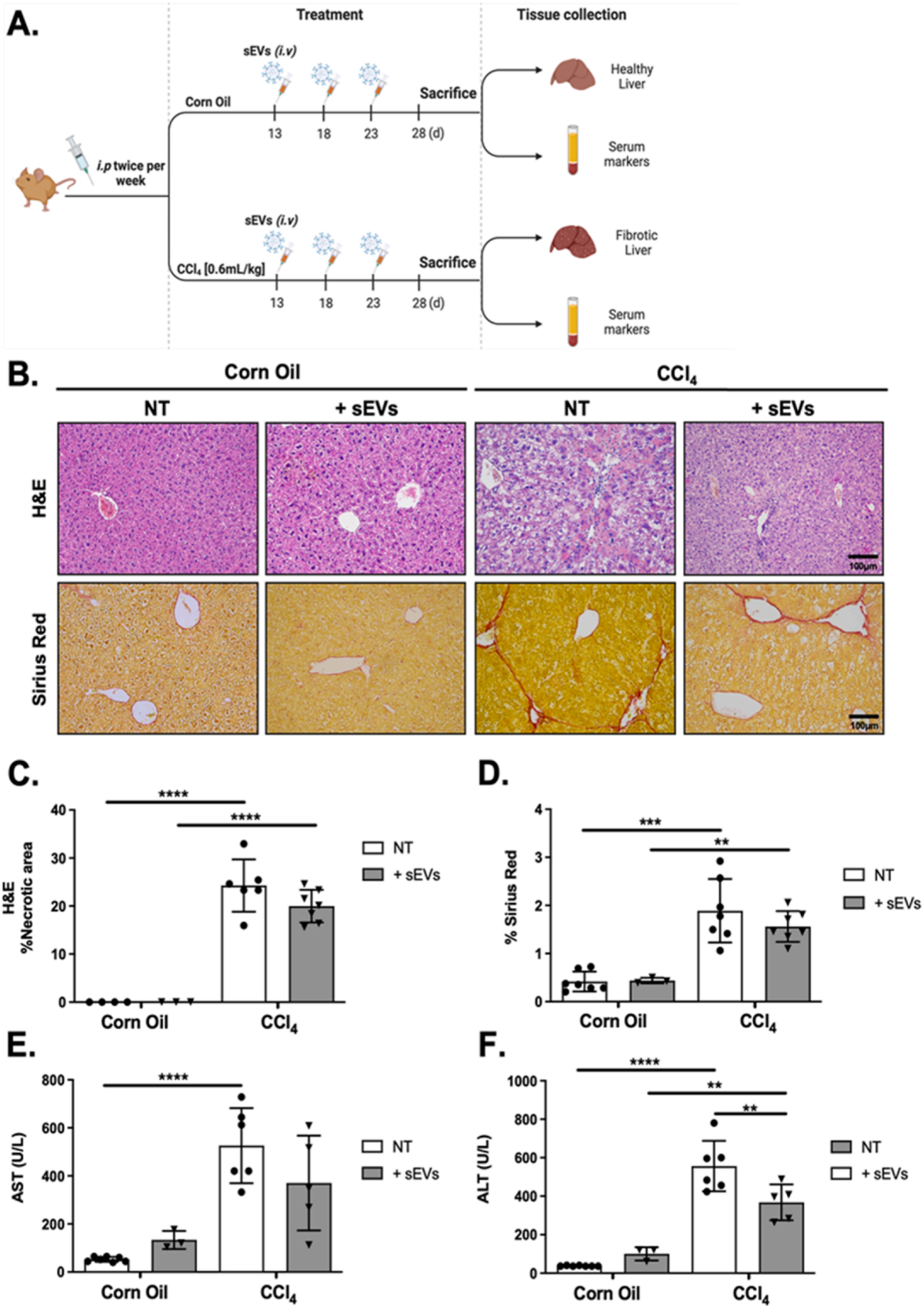

Fig. 7. A. Experimental scheme of *in vivo* evaluation of sEVCurAc in chronic liver injury model. B. H&E and Sirius red staining of control and CCl_4 treated mice with (+sEVs) or without (no treated, NT) sEVCurAc injection. C. Necrotic area quantification by H&E staining. D. % of fibrotic area quantification of SR staining. E. AST level assessment in serum. F. ALT values in serum. Data are expressed as mean ± SEM. *$p < 0.05$; **$p < 0.01$; ***$p < 0.001$; ****$p < 0.0001$ One-way ANOVA with post-hoc multiple comparisons test.

morphological modification of the sEV structure during the curcumin incorporation process, we employed two of the least invasive methodologies used in other similar synthetic NPs (liposomes): passive encapsulation in mild conditions (37ºC, PBS 1X pH 7.4) and active encapsulation in the presence of the detergent saponin, previously proposed for other liposome-like nanoparticles [32]. Both approaches confirmed the successful encapsulation of the drug with no membrane or structure alteration. Although both methods confirmed the encapsulation of the drug, three-fold higher yields of encapsulation were obtained by the active cargo method (sEVCurAc) [33,34]. However, for the clinical translation of our approach, further studies to reduce the concentrations of saponin should be considered due to the possible toxicity induced by this detergent [35]. To assess the release profile of the curcumin from our sEVCurAc system, a longitudinal evaluation was performed under physiological conditions. Although initial timepoints showed a slow release of the curcumin, main release occurred between 48 h and 216 h of study, with the maximum release at the longest study time (216 h). These outcomes suggest the possibility of reaching a sustained drug release. However, the release study did not show a plateau or stabilisation in the values, it would be interesting to evaluate longer times to determine the time at which the release of curcumin completes. This profile of drug release is similar to that described for other liposome-like systems [36]. Based on these results, we selected the compound sEVCurAc for further *in vitro* and *in vivo* evaluation.

In vitro evaluation of our nanosystem sEVCurAc by MTT assays, confocal microscopy and FC showed a diverse toxicity behaviour between curcumin-free sEVs (vehicles) and loaded sEVs. In all the cell lines tested, curcumin reduced the viability of all cell types in a dose- and time-dependent manner, being most noticeable in the cell lines RAW 264.7 and HepG2 compared to primary hepatocytes. These results suggest that loaded sEVs produce more intense damage to cells present in cancer environments, perhaps facilitating targeted therapy. Cytotoxicity assay and confocal microscopy results showed a high effect on RAW 264.7, which agrees with previous anti-inflammatory studies employing curcumin nanoemulsions in these same cells [37]. We observed a lower cytotoxic effect on HepG2 cells than on inflammatory cells (RAW 264.7) at the highest dose, which could be explained by the higher uptake of the nanosystem by the macrophages. This higher uptake in RAW 264.7 was also confirmed by FC and may be due to its natural function of eliminating foreign or harmful substances. Also, it is worth noting that RAW 264.7 cells are derived from mice and HepG2 cells from human, which may play a role in their uptake capacity due to their different metabolisms [38]. Although we have observed that primary hepatocytes were less affected by sEVCurAc, we could not perform FC assessment in primary hepatocytes because of the cell autofluorescence at the same wavelength as curcumin. The absence of significant changes in cell viability in presence of sEVs without curcumin confirmed that the cytotoxic effect was due to the curcumin encapsulated in the sEV structure. These data support the idea that the effect is due to the cargo and not to the sEV itself. Therefore, these results validate the innocuous effect of the sEVs and the therapeutic (anti-inflammatory and anti-tumour) effect of curcumin.

Regarding the distribution of DDS into the cell structure, confocal microscopy confirmed the incorporation of the sEVCurAc system into tumoral and inflammatory cell lines, with main cytoplasmatic distribution related to phago-lysosomal compartment [39], similar to other studies employing other nanoparticles as DDS of curcumin [40].

To evaluate the biodistribution of sEVCurAc, we performed an *in vivo* assessment by optical imaging. Longitudinal tracking of the fluorescent and curcumin-loaded sEVs showed a main liver uptake. Based on these results and previous studies [19,41,42], the last step of our work was the *in vivo* assessment of the therapeutic effect of our sEVCurAc as DDS in chronic acute liver disease induced by CCl_4. Histological evaluation of liver tissue in control models with sEVs and sEVCurAc showed no remarkable morphological changes, supporting the safety of our nanoplatforms. It has previously described the use of other water-soluble organic nanoparticles as curcumin-loaded vehicles to enhance curcumin-based therapy in models of CCl4-induced liver injury [43]. In the case of the CCl_4 model, treated group showed a significant reduction of serum makers of liver damage (eg: ALT levels), supporting the hepatoprotective biological role of curcumin in liver diseases [12]. A. Mahmoudi *et* al. described the target involvement of curcumin in nine potential genes linked to hepatopathology [44]. Histology images confirmed a tendency towards reduced in fibrogenesis as well as decreased necrotic area. Curcumin possesses therapeutic benefits These findings agreed with other research who reported that after treatment with curcumin, both serum markers and fibrosis area diminish in CCl_4 model [45–47]. Also, these results are in accordance with other studies suggesting that curcumin may be of future interest in hepatic fibrosis therapy specifically by modulating several intracellular signalling pathways in liver hepatic stellate cells (HSCs) [48,49]. Regarding the evaluation of other hepatoprotective markers such as NFR2 and NQO1, our results are in line with the literature and show that in a mouse model of CCl4-induced liver fibrosis there is indeed an increase in the expression and activity of both target genes of the antioxidant response. Furthermore, treatment with our sEVCurAc resulted in an increase in NQO1, an antioxidant response element, indicating enhanced antioxidant response. Nonetheless, the antifibrotic effect of sEVCurAc should be further tested in other models of chronic liver disease as well as using different doses and administration methodologies in order to find the optimal treatment conditions. Mechanistically, it is very likely that the antioxidant effect might help ameliorate the progression of hepatic fibrogenesis. Therefore, sEVCurAc might constitute a possible future treatment for patients with liver fibrosis.

5. Conclusions

We have developed a natural drug delivery system based on the encapsulation of curcumin into goatś milk sEVs, and confirmed the suitability of this DDS for being used as nanocarrier of hydrophobic drugs such as curcumin. Passive and active methodologies developed were tested and in all cases. The small extracellular vesicles maintained their original physicochemical properties after loading. Exosomal curcumin (sEVCurAc) produced cytotoxicity in cells, being more aggressive in stablished immortal cell lines (RAW 264.7 and HepG2) than in primary cells (primary hepatocytes). Also, sEVCurAc used as DDS were able to deliver to the liver and to ameliorate liver injury produced by CCl_4 reducing fibrotic deposits and transaminases levels.

Funding

This work was partially supported by Comunidad de Madrid (S2022/BMD-7403 RENIM-CM and EXOHEP2-CM (S2022/BMD-7409) and Ministerio de Ciencia, Innovación y Universidades, Instituto de Salud Carlos III (grant PI20/01632 and MICINN PID2020-117941RB-I00), co-financed by European Regional Development Fund (ERDF) (“A way of making Europe”). This work has been supported by European Union Horizon 2020 PRISMAP project and HORIZON-HLTH-2022-STAYHLTH-02 under agreement No 101095679. V. Albaladejo-García is grateful for financial support to Consejería de Educación e Investigación, co-financed by European Social Fund (ESF) grant PEJD-2018-PRE/BMD-9405. A. Santos-Coquillat grateful for financial support to Consejería de Educación e Investigación, co-financed by European Social Fund (ESF) grant PEJD-2018-POST/BMD-9592 and Sara Borrell Fellowship from Ministerio de Ciencia e Innovación, Instituto de Salud Carlos III grant CD19/00136. Funding for APC: Universidad Carlos III de Madrid (Agreement CRUE-Madroño 2024).

CRediT authorship contribution statement

Laura Morán: Writing – original draft, Investigation. **Virginia Albaladejo:** Writing – original draft, Investigation, Data curation.

Beatriz Salinas: Writing – review & editing, Writing – original draft, Supervision, Project administration, Methodology, Funding acquisition, Conceptualization. **Manuel Desco:** Writing – review & editing, Supervision, Investigation, Funding acquisition. **Francisco Javier Cubero:** Writing – review & editing, Supervision, Methodology. **Javier Vaquero:** Methodology. **Elena Vázquez:** Investigation. **Ye Hui:** Methodology, Investigation. **María Isabel González:** Methodology, Investigation. **Ana Santos Coquillat:** Methodology.

Declaration of Competing Interest

The authors declare the following financial interests/personal relationships which may be considered as potential competing interests: Manuel Desco & Beatriz Salinas reports financial support was provided by Community of Madrid. Beatriz Salinas reports financial support was provided by Spain Ministry of Science and Innovation. Beatriz Salinas reports financial support was provided by Carlos III Health Institute. Virgina Albaladejo & Ana Santos reports financial support was provided by Consejería de Educación e Investigación. Virginia Albaladejo & Ana Santos reports financial support was provided by European Social Fund. If there are other authors, they declare that they have no known competing financial interests or personal relationships that could have appeared to influence the work reported in this paper.

Acknowledgements

The authors gratefully thank Alexandra de Francisco, María de la Jara Felipe and Yolanda Sierra for their exceptional work with animal preparation. We are grateful to Laura Díaz from the Flow Cytometry and Sorter Unit, Maribel Clemente from the Cell Culture Unit and Rafael Samaniego from the Confocal Microscopy Unit, for the support received in support and counselling for the treatment and evaluation of cells. We also thank Marisa García Gil, from the Microscopy Unit of Centro Nacional de Microscopía Electrónica (CNME), for sample processing and image acquisition.

Appendix A. Supporting information

Supplementary data associated with this article can be found in the online version at doi:10.1016/j.biopha.2024.116381.

References

[1] S.K. Asrani, H. Devarbhavi, J. Eaton, P.S. Kamath, Burden of liver diseases in the world, J. Hepatol. vol. 70 (1) (Jan 2019) 151–171, https://doi.org/10.1016/j.jhep.2018.09.014.
[2] R. Bataller, D.A. Brenner, Liver fibrosis, J. Clin. Invest vol. 115 (2) (Feb 2005) 209–218, https://doi.org/10.1172/jci24282.
[3] H. Cichoż-Lach, A. Michalak, Oxidative stress as a crucial factor in liver diseases, World J. Gastroenterol. vol. 20 (25) (Jul 2014) 8082–8091, https://doi.org/10.3748/wjg.v20.i25.8082.
[4] K. Reyes-Gordillo, R. Shah, M.R. Lakshman, R.E. Flores-Beltrán, P. Muriel, Chapter 49 - Hepatoprotective Properties of Curcumin, in: P. Muriel (Ed.), Liver Pathophysiology, Academic Press,, Boston, 2017, pp. 687–704, https://doi.org/10.1016/B978-0-12-804274-8.00049-7.
[5] D. Sun, et al., A novel nanoparticle drug delivery system: the anti-inflammatory activity of curcumin is enhanced when encapsulated in exosomes, Mol. Ther. vol. 18 (9) (Sep 2010) 1606–1614, https://doi.org/10.1038/mt.2010.105.
[6] R. Afrin, et al., Curcumin ameliorates liver damage and progression of NASH in NASH-HCC mouse model possibly by modulating HMGB1-NF-κB translocation, Int Immunopharmacol. vol. 44 (Mar 2017) 174–182, https://doi.org/10.1016/j.intimp.2017.01.016.
[7] S. Rong, et al., Curcumin prevents chronic alcohol-induced liver disease involving decreasing ROS generation and enhancing antioxidative capacity, Phytomedicine vol. 19 (6) (Apr 2012) 545–550, https://doi.org/10.1016/j.phymed.2011.12.006.
[8] D. Cerný, et al., Hepatoprotective effect of curcumin in lipopolysaccharide/-galactosamine model of liver injury in rats: relationship to HO-1/CO antioxidant system, Fitoterapia vol. 82 (5) (Jul 2011) 786–791, https://doi.org/10.1016/j.fitote.2011.04.003.
[9] F.F. Cox, et al., Protective Effects of Curcumin in Cardiovascular Diseases-Impact on Oxidative Stress and Mitochondria, Cells vol. 11 (3) (Jan 2022) 342, https://doi.org/10.3390/cells11030342.
[10] R. Pluta, M. Ułamek-Kozioł, S.J. Czuczwar, Neuroprotective and neurological/cognitive enhancement effects of curcumin after brain ischemia injury with Alzheimer's disease phenotype, Int J. Mol. Sci. vol. 19 (12) (Dec 2018), https://doi.org/10.3390/ijms19124002.
[11] A. Giordano, G. Tommonaro, Curcumin and cancer, Nutrients vol. 11 (10) (Oct 2019), https://doi.org/10.3390/nu11102376.
[12] M.H. Farzaei, et al., Curcumin in liver diseases: a systematic review of the cellular mechanisms of oxidative stress and clinical perspective, Nutrients vol. 10 (7) (Jul 2018) 855, https://doi.org/10.3390/nu10070855.
[13] P. Anand, A.B. Kunnumakkara, R.A. Newman, B.B. Aggarwal, Bioavailability of curcumin: problems and promises, Mol. Pharm. vol. 4 (6) (Nov-Dec 2007) 807–818, https://doi.org/10.1021/mp700113r.
[14] B. Sinjari, et al., Curcumin/liposome nanotechnology as delivery platform for anti-inflammatory activities via NFkB/ERK/pERK pathway in human dental pulp treated with 2-hydroxyethyl methacrylate (HEMA), Front Physiol. vol. 10 (Jun 2019) 633, https://doi.org/10.3389/fphys.2019.00633.
[15] S. Ghosh, S. Dutta, A. Sarkar, M. Kundu, P.C. Sil, Targeted delivery of curcumin in breast cancer cells via hyaluronic acid modified mesoporous silica nanoparticle to enhance anticancer efficiency, Colloids Surf. B Biointerfaces vol. 197 (Jan 2021) 111404, https://doi.org/10.1016/j.colsurfb.2020.111404.
[16] Y. Zhang, Y. Liu, H. Liu, W.H. Tang, Exosomes: biogenesis, biologic function and clinical potential, Cell Biosci. vol. 9 (1) (Feb 2019) 19, https://doi.org/10.1186/s13578-019-0282-2.
[17] H. Valadi, K. Ekström, A. Bossios, M. Sjöstrand, J.J. Lee, J.O. Lötvall, Exosome-mediated transfer of mRNAs and microRNAs is a novel mechanism of genetic exchange between cells, Nat. Cell Biol. vol. 9 (6) (Jun 2007) 654–659, https://doi.org/10.1038/ncb1596.
[18] M.I. Gonzalez, P. Martin-Duque, M. Desco, B. Salinas, Radioactive Labeling of Milk-Derived Exosomes with (99m)Tc and In Vivo Tracking by SPECT Imaging, Nanomater. (Basel) vol. 10 (6) (May 2020) 1062, https://doi.org/10.3390/nano10061062.
[19] A. Santos-Coquillat, et al., Goat milk exosomes as natural nanoparticles for detecting inflammatory processes by optical imaging, https://doi.org/10.1002/smll.202105421, Small vol. 18 (6) (Feb 2022) 2105421, https://doi.org/10.1002/smll.202105421.
[20] V. Sengupta, S. Sengupta, A. Lazo, P. Woods, A. Nolan, N. Bremer, Exosomes derived from bone marrow mesenchymal stem cells as treatment for severe COVID-19, Stem Cells Dev. vol. 29 (12) (Jun 2020) 747–754, https://doi.org/10.1089/scd.2020.0080.
[21] X. Luan, K. Sansanaphongpricha, I. Myers, H. Chen, H. Yuan, D. Sun, Engineering exosomes as refined biological nanoplatforms for drug delivery, Acta Pharm. Sin. vol. 38 (6) (Jun 2017) 754–763, https://doi.org/10.1038/aps.2017.12.
[22] W. Liao, et al., Exosomes: The next generation of endogenous nanomaterials for advanced drug delivery and therapy, Acta Biomater. vol. 86 (Mar 2019) 1–14, https://doi.org/10.1016/j.actbio.2018.12.045.
[23] C. Nedeva, S. Mathivanan, Engineering extracellular vesicles for cancer therapy, Subcell. Biochem vol. 97 (Mar 2021) 375–392, https://doi.org/10.1007/978-3-030-67171-6_14.
[24] B. Adriano, N.M. Cotto, N. Chauhan, M. Jaggi, S.C. Chauhan, M.M. Yallapu, Milk exosomes: nature's abundant nanoplatform for theranostic applications, Bioact. Mater. vol. 6 (8) (Aug 2021) 2479–2490, https://doi.org/10.1016/j.bioactmat.2021.01.009.
[25] E. van der Pol, A.N. Böing, P. Harrison, A. Sturk, R. Nieuwland, Classification, functions, and clinical relevance of extracellular vesicles, Pharm. Rev. vol. 64 (3) (Jul 2012) 676–705, https://doi.org/10.1124/pr.112.005983.
[26] P.G. Moon, S. You, J.E. Lee, D. Hwang, M.C. Baek, Urinary exosomes and proteomics, Mass Spectrom. Rev. vol. 30 (6) (Nov-Dec 2011) 1185–1202, https://doi.org/10.1002/mas.20319.
[27] M.I. González, et al., Covalently labeled fluorescent exosomes for in vitro and in vivo applications, Biomedicines vol. 9 (1) (Jan 2021) 81, https://doi.org/10.3390/biomedicines9010081.
[28] S.G. Antimisiaris, S. Mourtas, A. Marazioti, Exosomes and exosome-inspired vesicles for targeted drug delivery, Pharmaceutics vol. 10 (4) (2018) 218, https://doi.org/10.3390/pharmaceutics10040218.
[29] M.J. Haney, N.L. Klyachko, E.B. Harrison, Y. Zhao, A.V. Kabanov, E.V. Batrakova, TPP1 delivery to lysosomes with extracellular vesicles and their enhanced brain distribution in the animal model of batten Disease, Adv. Health Mater. vol. 8 (11) (Jun 2019) e1801271, https://doi.org/10.1002/adhm.201801271.
[30] D.H. Kim, et al., Noninvasive assessment of exosome Pharmacokinetics In Vivo: A Review, Pharmaceutics vol. 11 (12) (Nov 2019) 649, https://doi.org/10.3390/pharmaceutics11120649.
[31] R. Munagala, F. Aqil, J. Jeyabalan, R.C. Gupta, Bovine milk-derived exosomes for drug delivery, Cancer Lett. vol. 371 (1) (Feb 2016) 48–61, https://doi.org/10.1016/j.canlet.2015.10.020.
[32] G. Fuhrmann, A. Serio, M. Mazo, R. Nair, M.M. Stevens, Active loading into extracellular vesicles significantly improves the cellular uptake and photodynamic effect of porphyrins, J. Control Release vol. 205 (May 2015) 35–44, https://doi.org/10.1016/j.jconrel.2014.11.029.
[33] M. Sancho-Albero, et al., Efficient encapsulation of theranostic nanoparticles in cell-derived exosomes: leveraging the exosomal biogenesis pathway to obtain hollow gold nanoparticle-hybrids, Nanoscale vol. 11 (40) (Oct 2019) 18825–18836, https://doi.org/10.1039/c9nr06183e.
[34] F. Ahmed, M. Tamma, U. Pathigadapa, P. Reddanna, V.R. Yenuganti, drug loading and functional efficacy of cow, buffalo, and goat milk-derived exosomes: a comparative study, Mol. Pharm. vol. 19 (3) (Mar 2022) 763–774, https://doi.org/10.1021/acs.molpharmaceut.1c00182.

[35] R. Bissinger, et al., Effect of saponin on erythrocytes, Int. J. Hematol. vol. 100 (1) (Jul 2014) 51–59, https://doi.org/10.1007/s12185-014-1605-z.
[36] X. Zhang, Y. Wang, Y. Zhao, L. Sun, pH-responsive drug release and real-time fluorescence detection of porous silica nanoparticles, Mater. Sci. Eng. C. Mater. Biol. Appl. vol. 77 (Aug 2017) 19–26, https://doi.org/10.1016/j.msec.2017.03.224.
[37] N.A. Young, et al., Oral administration of nano-emulsion curcumin in mice suppresses inflammatory-induced NFκB signaling and macrophage migration, PLOS ONE vol. 9 (11) (Nov 2014) e111559, https://doi.org/10.1371/journal.pone.0111559.
[38] C.H.C. Leenaars, et al., Animal to human translation: a systematic scoping review of reported concordance rates, J. Transl. Med vol. 17 (1) (Jul 2019) 223, https://doi.org/10.1186/s12967-019-1976-2.
[39] P.S. Jahagirdar, P.K. Gupta, S.P. Kulkarni, P.V. Devarajan, Polymeric curcumin nanoparticles by a facile in situ method for macrophage targeted delivery, Bioeng. Transl. Med vol. 4 (1) (Jan 2019) 141–151, https://doi.org/10.1002/btm2.10112.
[40] M. Vashisht, P. Rani, S.K. Onteru, D. Singh, Curcumin Encapsulated in Milk Exosomes Resists Human Digestion and Possesses Enhanced Intestinal Permeability in Vitro, Appl. Biochem Biotechnol. vol. 183 (3) (Nov 2017) 993–1007, https://doi.org/10.1007/s12010-017-2478-4.
[41] S.M. Hirst, et al., Bio-distribution and in vivo antioxidant effects of cerium oxide nanoparticles in mice, Environ. Toxicol. vol. 28 (2) (Feb 2013) 107–118, https://doi.org/10.1002/tox.20704.
[42] J. Duan, et al., Synthesis and in vitro/in vivo anti-cancer evaluation of curcumin-loaded chitosan/poly(butyl cyanoacrylate) nanoparticles, Int J. Pharm. vol. 400 (1-2) (Nov 2010) 211–220, https://doi.org/10.1016/j.ijpharm.2010.08.033.
[43] S. Bisht, M.A. Khan, M. Bekhit, H. Bai, T. Cornish, M. Mizuma, M.A. Rudek, M. Zhao, A. Maitra, B. Ray, D. Lahiri, A. Maitra, R.A. Anders, A polymeric nanoparticle formulation of curcumin (NanoCurc™) ameliorates CCl4-induced hepatic injury and fibrosis through reduction of pro-inflammatory cytokines and stellate cell activation, Lab Invest vol. 91 (9) (Sep 2011) 1383–1395, https://doi.org/10.1038/labinvest.2011.86.
[44] Y. Zhao, X. Ma, J. Wang, X. He, Y. Hu, P. Zhang, R. Wang, R. Li, M. Gong, S. Luo, S, X. Xiao, Curcumin protects against CCl4-induced liver fibrosis in rats by inhibiting HIF-1α through an ERK-dependent pathway, Molecules vol. 19 (11) (Nov 2014) 18767–18780, https://doi.org/10.3390/molecules191118767.
[45] A. Mahmoudi, S.L. Atkin, T. Jamialahmadi, M. Banach, A. Sahebkar, Effect of curcumin on attenuation of liver cirrhosis via genes/proteins and pathways: a system pharmacology study, Nutrients vol. 14 (20) (Oct 2022) 4344, https://doi.org/10.3390/nu14204344.
[46] M.A. Abo-Zaid, E.S. Shaheen, A.H. Ismail, Immunomodulatory effect of curcumin on hepatic cirrhosis in experimental rats, J. Food Biochem vol. 44 (6) (Jun 2020) e13219, https://doi.org/10.1111/jfbc.13219.
[47] Y. Fu, S. Zheng, J. Lin, J. Ryerse, A. Chen, Curcumin protects the rat liver from CCl4-caused injury and fibrogenesis by attenuating oxidative stress and suppressing inflammation, 2008, Mol. Pharm. vol. 73 (2) (Feb 2008) 399–409, https://doi.org/10.1124/mol.107.039818.
[48] M.A. O'Connell, S.A. Rushworth, Curcumin: potential for hepatic fibrosis therapy? Br. J. Pharm. vol. 153 (3) (Feb 2008) 403–405, https://doi.org/10.1038/sj.bjp.0707580.
[49] A.R. Buonomo, R. Scotto, S. Nappa, M. Arcopinto, A. Salzano, A.M. Marra, R. D'Assante, E. Zappulo, G. Borgia, I. Gentile, The role of curcumin in liver diseases, Arch. Med Sci. vol. 15 (6) (Oct 2019) 1608–1620, https://doi.org/10.5114/aoms.2018.73596.